https://doi.org/10.5194/ar-2026-9
Preprint. Discussion started: 16 February 2026


AEROSOL Research Discussions

# Coral reef exposure increases aerosol and cloud condensation nuclei over the Great Barrier Reef

Juha Sulo[1]*, Magdalena Okuljar[1]*, Joel Alroe[1], Zijun Li[1], Eva Johanna Horchler[1]**, Luke Cravigan[1], Branka Miljevic[1], Luke Harrison[2], Daniel Harrison[2], Zoran Ristovski[1]

[1] School of Earth and Atmospheric Sciences, Queensland University of Technology, Brisbane, Australia

[2]Reefs and Oceans Research Cluster, National Marine Science Centre, Southern Cross University, Coffs Harbour, NSW, Australia

* The first and second author contributed equally to this work

** Now at Department of Chemistry, Aarhus University, Aarhus, Denmark

Correspondence to: Juha Sulo, email: juha.sulo@qut.edu.au

**Abstract.** The Great Barrier Reef (GBR) is the largest reef ecosystem in the world and a home to diverse marine life. Lower troposphere aerosol concentrations and dynamics over the GBR are important for cloud and radiative processes, however their in-situ characterisation is lacking in the literature. In this study, we present analysis of multi-year in situ aerosol measurements over the GBR, showing for the first time direct observations of coral reefs contributing to aerosol loading over the reef. Our results show that aerosol concentrations over the GBR are typical of a clean coastal environment, and the aerosol loading over the GBR is primarily influenced by long-range transport of aerosol particles. However, a non-negligible effect from local sources is also observed. The fraction of ultrafine particles in the aerosol population increases in air masses that pass over the coral reef ecosystem. Our statistical modelling shows that cloud condensation nuclei concentrations over the GBR are dominantly driven by availability of accumulation and Aitken mode aerosol particles with negligible effects from local meteorology. While accumulation mode particle concentrations have the strongest impact on cloud condensation nuclei concentrations, counterfactual modelling shows that Aitken mode concentrations can contribute up to 6% of cloud condensation nuclei over the reef.

## 1 Introduction

Coral reefs are one of the most diverse ecosystems in the world, home to more than 25% of all marine life while covering less than one percent of the ocean floor (Knowlton et al., 2010; Reaka, 1997). Globally, coral reefs offer protection to coastlines from extreme weather events (Harris et al., 2018), job opportunities to nearby communities, and recreational opportunities to locals and tourists alike (Santavy et al., 2021). The Great Barrier Reef (GBR) is the largest reef ecosystem in the world, and an important cultural site for indigenous Australians (Rowland et al., 2025). However, coral reefs are under severe stress from multiple stressors, including increased ocean temperatures and extreme weather events, ocean acidification, and habitat destruction by humans (Dietzel et al., 2021; Hughes et al., 2017b, a). The increase in ocean temperatures is associated with a

https://doi.org/10.5194/ar-2026-9
Preprint. Discussion started: 16 February 2026


AEROSOL Research Discussions

corresponding increase in surface-intensified warming (Fox-Kemper et al., 2021). Furthermore, coral bleaching is primarily caused by heat stress from increased sea water temperature and irradiative stress from UV radiation (Berkelmans, 2002; Brown, 1997; Courtial et al., 2017). The GBR has seen an increasing frequency of mass coral bleaching events, with severe and prevalent mass bleaching events observed on approximately 40 % of the reefs nearly every year since 2020 (Australian Institute for Marine Science, 2025; Hughes et al., 2017b).

Aerosol particles can attenuate temperature and radiation extremes both directly by scattering light as well as via aerosol-cloud interactions. Combined aerosol-radiation and aerosol-cloud interactions are estimated to have a -1.3 W $m^{-2}$ [-2.0 to -0.6] W $m^{-2}$ net effective anthropogenic radiative forcing on the global energy budget, which has masked around one third of continental warming from greenhouse gases (Storelvmo et al., 2016). Cloud properties are modified by the availability and concentration of cloud condensation nuclei (CCN) as well as precursor aerosol. Due to its remote location, aerosol dynamics over the GBR have been mostly studied by satellite measurements and modelling (Cropp et al., 2018; Fiddes et al., 2022; Jackson et al., 2018; Swan, 2022). Many of the studies also focus on the potential of marine dimethyl sulfide (DMS) as a precursor for non-sea salt sulfate and new aerosol particles as part of the CLAW (Charlson, Lovelock, Andreae and Warren) hypothesis (Swan et al., 2016). The CLAW hypothesis proposes a negative feedback loop that links ocean warming due to increase in solar irradiance with higher emissions of DMS and subsequent new particle formation (NPF) leading to increase in CCN concentration and cloud albedo. Condensable vapours such as oxidation products of DMS can also contribute to aerosol growth and loading without ongoing NPF process. However, in-situ measurements characterizing lower troposphere aerosol concentrations and dynamics over the GBR are lacking in literature. Month-long field campaigns with limited instrumentation and case studies have been reported, showing that local source contribution to the ambient aerosol population such as new particle formation or primary emissions from biogenic or anthropogenic sources is possible (Modini et al., 2009; Swan et al., 2016; Vaattovaara et al., 2014). However, this contribution has not been quantified using robust in-situ measurements for long-term effects or magnitude.

Fiddes et al. (2022) argued in their modelling study that reef sources likely do not contribute meaningfully to increased aerosol number concentration due to the prevalence of anthropogenic sulfur-containing compounds over the reef from the Queensland coast but rather may contribute to increased aerosol mass or size. Earlier aerosol measurements by Modini et al. (2009) detected NPF in air masses that passed over the GBR, but the aerosol source was left uncertain. Furthermore, there are currently no in situ studies characterizing spatiotemporal aerosol variations over the GBR.

In this study, we characterize the spatiotemporal variation of aerosol concentrations over the GBR and quantify the drivers behind CCN concentrations using eight months of in situ data collected using mobile and stationary platforms over the span of eight years. Lastly, we investigate variability in cloud processing and local aerosol particle sources over the GBR. Assessing background aerosol concentrations and their dynamics over the GBR is an objective of the Reef Restoration and Adaptation Program (RRAP) Cooling and Shading subprogram, which investigates technologies to mitigate bleaching stress on coral reefs. Atmospheric interventions being investigated by the program include reducing the amount of downwelling solar radiation through generating artificial sea fog and marine cloud brightening (Harrison, 2024; Hernandez-Jaramillo et al., 2025; Li et al.,

https://doi.org/10.5194/ar-2026-9
Preprint. Discussion started: 16 February 2026




2025). Quantifying lower troposphere aerosol concentrations, their sources, spatiotemporal variability and capacity to act as CCN are key steps in understanding aerosol-cloud-radiation dynamics over the reef environment. Furthermore, they are important in understanding the baseline conditions over the reef for attempting any solar radiation management interventions to protect the reef from bleaching.

## 2 Methods

### 2.1 Measurement campaigns

Over the last decade, there have been multiple atmospheric measurement campaigns to understand different aspects of the atmosphere over the GBR. These campaigns have large spatial variability along the reef, and different parts of the reef have been monitored over different years (Fig. S1). An overview of the campaign datasets used in this study is shown in Table 1. The Reef to Rainforest (R2R) campaign in 2016 studied the effects of the GBR itself on cloud properties and rain. The 2019 dataset represents opportunistic measurements captured during a transit voyage for the RV Investigator from Brisbane to Darwin. The remaining campaigns since 2021 have been part of the RRAP Cooling and Shading Program focused on an effort to protect the reef corals from heat and light stress, a core component of which is to improve fundamental understanding of meteorological, aerosol, and cloud microphysical processes over the GBR (Braga et al., 2025; Deschaseaux et al., 2025; Eckert et al., 2023, 2024; Hernandez-Jaramillo et al., 2024; Richards et al., 2024; Ryan et al., 2024; Zhao et al., 2024). Overall, these campaigns represent both stationary measurements and longer voyage tracks, with a greater density in the southern and central reef.

Table 1. Overview of campaigns used in this study.

| Starting date | Ending date | Coordinates (°N, °E) | Type of campaign |
|---|---|---|---|
| 2016-09-29 | 2016-10-23 | Starting: - 16.95, 145.97<br>Ending: -24.50, 153.73 | R2R Shipborne: Investigator (IN05) |
| 2019-10-05 | 2019-10-10 | Starting: -24.48, 153.93<br>Ending: -10.44, 142.55 | Transit voyage Shipborne: Investigator (T02) |
| 2021-03-14 | 2021-03-24 | -18.85, 147.72 | Stationary: Broadhurst reef |
| 2021-12-04 | 2021-12-16 | Starting: -18.85, 147.69<br>Ending: -18.66, 147.70 | Shipborne: Magnetic, Guardian |
| 2022-02-08 | 2022-04-01 | Starting: -18.90, 147.70<br>Ending: -19.26, 146.83 | Shipborne: Magnetic, Guardian |
| 2023-02-17 | 2023-03-27 | -23.44, 151.91 | Stationary: Heron Island |

### 2.2 Measurements

Measurements used in this study include comprehensive measurements of the physical and meteorological properties of the atmosphere over the GBR. The variables used in the general spatiotemporal characterisation were narrowed down to those that appear in each measurement campaign, providing maximum spatial and temporal coverage. An overview of variables used in

https://doi.org/10.5194/ar-2026-9
Preprint. Discussion started: 16 February 2026


AEROSOL Research Discussions

the analysis is listed in Table S1. The dataset was harmonized to a time resolution of 15 minutes, with median values used for aggregating data with a higher time resolution.

Aerosol particle number concentration was measured using a condensation particle counter (CPC, Brechtel, USA or Airmodus, Finland or TSI, USA) with a cutoff of 10 nm ($N_{tot}$) and the aerosol number size distribution was measured using a Scanning Mobility Particle Sizer (SMPS, TSI, USA) or Scanning Electrical Mobility Spectrometer (SEMS, Brechtel, USA) and an Aerodynamic Particle Size (APS, TSI, USA), covering a combined size range between 10 and 5000 nm. Particle number concentrations were calculated for nucleation mode (under 20 nm), Aitken mode (20 – 80 nm), accumulation mode (80 – 1000 nm), and coarse mode (1000 – 5000 nm). In addition, the CCN concentration was measured using a CCN-100 counter (Droplet Measurement Technologies, USA). In some of the campaigns, CCN concentration was measured using a single supersaturation level of 0.5% only, and therefore, for the spatiotemporal analysis, CCN concentration at 0.5% supersaturation was chosen as indicative of CCN concentrations in the entire dataset.

Meteorological variables were measured with a number of different weather stations and instruments. Campaigns in 2016 and 2019 used the RV Investigator's built-in suite of weather sensors. The March 2021 campaign utilized the WS800-UMB weather station (Lufft, Germany), and subsequent campaigns used the MaxiMet GMX501 (Gill Instruments Ltd., UK). Temperature, pressure, relative humidity, solar irradiance, and wind direction and speed were measured in each campaign. Auxiliary measurements like precipitation and dew point temperature were only available in some campaign datasets and were not used in the analysis.

Black carbon concentration was measured using an aethalometer (AE31, Aerosol Magee Scientific, Slovenia) or Tricolour Absorption Photometer (TAP, Brechtel, USA) with red wavelength. The two instruments have been shown to agree fairly well in temporal variation, although the absolute values have discrepancies depending on the correction algorithms chosen (Laing et al., 2020). Black carbon concentration was used for determining episodes during which the measured ambient air was contaminated by local pollution sources such as the ship plume from the RV Investigator or diesel engine sources on Heron Island. The RV Investigator uses its own algorithm for detecting when the ship plume is affecting its measurements (Humphries et al., 2019). For shipborne RRAP campaigns, we removed data points during which the winds originated from the aft sector (90° – 270° relative to the ship's heading) and the black carbon concentration was above 30 ng/m$^3$. For the Heron Island campaign, the limit for black carbon was increased to 50 ng/m$^3$, representing elevated background concentrations due to co-located infrastructure at the island-based sampling site. The specific limits were selected to exclude outliers, identified as values that exceeded the 95$^{th}$ quantile in the datasets.

### 2.3 Calculations

Several derived parameters were calculated from the available datasets to support further analysis. The Hoppel minimum (Hoppel et al., 1985; Noble and Hudson, 2019), the diameter of minimum concentration between the Aitken and accumulation modes was calculated by fitting a smoothing spline on the size distribution between 40 and 140 nm and finding the minimum concentration diameter. In case the minimum concentration was not found within this size limit or it was found at the edge of

https://doi.org/10.5194/ar-2026-9
Preprint. Discussion started: 16 February 2026




it, the size distribution was considered monomodal in terms of Aitken and accumulation mode, and the Hoppel minimum value was marked as missing. A subsequent Hoppel minimum value was constrained by the previous value, based on the assumption that a Hoppel minimum diameter varying more than 10 nm either way in 15 minutes would either be unrealistic or a sign of a rapid change of airmass.

The critical diameter is the particle diameter above which particles are assumed to be active as CCN. Here, we defined it as the diameter above which the number concentration of the size distribution and the total CCN concentration reach unity (Sihto et al., 2011), and it was calculated for every data point in which aligned CCN and size distribution data were available. This method of calculating critical diameter assumes that activation of atmospheric particles as CCN depends only on particle size, not chemical composition, under the assumption of a fully internal mixture of aerosol particles. This likely leads to higher uncertainty in critical diameter as ambient aerosol particles have a more complex mixing state (Riemer et al., 2019). The hygroscopicity parameter kappa (Petters and Kreidenweis, 2007) was calculated based on the dry critical diameter for the datasets that contained CCN concentrations measured with varying supersaturation. CCN activation ratio, defined as the ratio between CCN and total aerosol number concentrations was calculated whenever data was available. For consistency, the CCN concentrations at 0.5% supersaturation were considered. Because the real supersaturation in the atmosphere is likely to vary (Krüger et al., 2014), CCN concentration, critical diameter, activation ratio, and kappa have inherently more uncertainties than other measured variables in the dataset.

In order to determine the effect of both continental and reef sources on the airmasses, 72-hour back trajectories were calculated per hour using the HYSPLIT (Stein et al., 2015) Lagrangian dispersion model by the National Oceanic and Atmospheric Administration (NOAA), matching the latitude, longitude and time for each in-situ data point. The Global Data Assimilation System (GDAS) dataset at 1° spatial resolution provided by NOAA was used for HYSPLIT analysis. The land fraction was defined as the fraction of times during which HYSPLIT output coordinates placed the airmass over land and below a conservative boundary layer threshold—defined as the HYSPLIT planetary boundary layer height plus one standard deviation. The definition for being on land or over ocean was based on the centroids of the grid cell. The reef fraction was calculated in a similar manner by using the coordinates of the GBR reef lagoon (Great Barrier Reef Marine Park Authority, 2007). Low and total cloud coverage from ERA5 reanalysis data with 1-hour time resolution (Hersbach et al., 2023) was used as supporting variables in the analysis. The reanalysis product combines satellite and ground-based measurements, generating a data product with a spatial resolution of 0.25°, or roughly 31x31 km at the GBR. The data retrieved from ERA5 and airmass back trajectories were forward-filled to a 15-minute resolution. The variables used from these sources typically vary in time scales larger than 15 minutes, and forward filling avoids artifacts from other interpolation methods. This was done to allow merging 1-hour data with 15-minute in situ measurements. While forward-filling does not generate sub-hourly structure, ERA5 reanalysis does not contain physically meaningful sub-hourly information for these variables. Any other interpolation method would necessarily introduce synthetic variability; therefore forward-filling is the most conservative choice.

Gradient boosting regression algorithm from the scikit-learn Python package (Friedman, 2001; Pedregosa et al., 2011) was used to construct a predictive model and help determine which features of the dataset best explain CCN concentrations at the

https://doi.org/10.5194/ar-2026-9
Preprint. Discussion started: 16 February 2026




GBR. The gradient boosting algorithm is an ensemble method, using several base estimators to build a decision tree in a step-by-step fashion, aiming to minimize the overall prediction error at each addition (Friedman, 2001). The gradient boosting hyperparameters were tuned by performing an exhaustive grid search in the hyperparameter space (Yang and Shami, 2020), using 5-fold cross-validation and a base regression with a learning rate of 0.1, 250 estimators and a minimum sample split of 2 as scoring estimator. Friedman mean squared error (MSE; Friedman, 2001) was used as the metric for split quality in building the regression model. Feature selection was done by using permutation feature importance (Adler and Painsky, 2022; Breiman, 2001; Doshi-Velez and Kim, 2017) with 10,000 repetitions. The directionality of the selected features were tested using Shapley Additive Explanations (SHAP) values (Lundberg and Lee, 2017) and partial dependence plots (Friedman, 2001).

We quantified the conditional effect of Aitken-mode aerosols on CCN concentrations using a counterfactual modelling framework. Counterfactual analysis (Manshausen et al., 2022; Marelle et al., 2025) estimates how the predicted variable of a model changes if a single predictor is altered while all other conditions remain constant. This allows for isolating the modelled contribution of specific variables under consistent meteorological and compositional contexts. We trained a gradient boosting model as described above. The model was fitted to all available observations, with predictor variables representing aerosol size distributions, composition, and concurrent meteorological conditions. The trained model was then used to generate two sets of predictions: baseline predictions, using the observed feature values, and counterfactual predictions, where the Aitken mode particle concentration was fixed to the 1st percentile of its distribution. The resulting difference ($\Delta$CCN = baseline − counterfactual) represents the modelled change in CCN concentration under a hypothetical regime of minimal Aitken-mode aerosol abundance. Uncertainty in $\Delta$CCN was estimated using a batch bootstrap procedure that resampled contiguous temporal segments, defined by data gaps exceeding one hour, to preserve the serial correlation structure typical of atmospheric time series. This resampling approach produced 95% confidence intervals for the mean and median $\Delta$CCN based on 10,000 replicates.

### 2.4 Uncertainty of analysis

There are a number of uncertainties related to our analysis. The uneven spatial and temporal distribution of the data makes it difficult to infer spatiotemporal variability in the analysis. Years 2021-2023 occurred during the four-year La Nina event from 2020 to 2023, while 2016 was an El Niño year and 2019 was a neutral El Niño Southern Oscillation (ENSO). The different phases of ENSO likely contribute to the increased variability in our measurements, as variations in ENSO affect not only the meteorology and precipitation over the reef, but also sea surface temperatures. Additionally, a lack of reliable measurements in the nucleation mode range and a lack of sub-10 nm altogether make accounting for local sources more demanding. Lastly, CCN concentrations in the dataset are measured at 0.5% water supersaturation, but the typical supersaturation level over GBR is likely variable and lower than 0.5 % (Horchler et al., 2025). This can lead to an overestimation of the CCN concentration and activation ratio in the dataset and consequently underestimation of critical diameter. Disentangling temporal and spatial variability over the reef requires dedicated multiyear measurements in a single location, as well as ideally a period of spatially distributed simultaneous measurements. However, since there has never been any co-ordinated, continuous multi-year

https://doi.org/10.5194/ar-2026-9
Preprint. Discussion started: 16 February 2026




atmospheric composition monitoring over the GBR prior to RRAP, such datasets do not currently exist. Furthermore, our analysis does not address the potential for chemical information to reveal more about the sources of the aerosol that exist over the reef. Although vapor emissions from coral reefs have been studied before, aerosol chemical composition, particularly in combination with analysis on vapor emissions over the reef, are lacking in current literature. Finally, more detailed investigation into apparent in-cloud supersaturation and the dynamics of atmospheric convection over the reef are needed to properly characterize cloud formation and the role of CCN over the GBR.

## 3 Results

### 3.1 Overview of meteorological parameters and aerosol population over GBR

Overall, meteorological parameters over the GBR are representative of a subtropical marine environment, indicating a warm, humid environment (most commonly at ~80%) mostly influenced by marine airmasses advecting from east to south-east (Fig. S2). Solar irradiance often peaks around 1000 W/m$^2$, and low cloud cover fraction on the reef is typically relatively low (Fig. S2d, i), confirming that trade wind cumulus cloud fields tend to dominate over the GBR (Coddington et al., 2016; Zhao et al., 2022). $N_{tot}$ is typically between 100 and 800 cm$^{-3}$ (Fig. 1a). These concentrations are all consistent with a clean coastal environment with a mix of different sources in the Southern Hemisphere (Humphries et al., 2021; Law et al., 2017; Peltola et al., 2022), while aerosol particle number concentrations in remote marine environments are typically reported as being below 200 cm$^{-3}$ (Ansmann et al., 2023; Humphries et al., 2023).

Mode values of $N_{tot}$ (500 cm$^{-3}$), CCN concentration (250 cm$^{-3}$), accumulation mode (80 – 1000 nm) particle concentration (120 cm$^{-3}$), and Hoppel minimum (70 nm) are comparable between most datasets (Fig. 1a,b,e,f). However, March 2021 campaign dataset stands out as an exception, exhibiting generally lower aerosol number concentrations but higher activation ratio, critical diameter and Hoppel minimum (Fig. 1c,d,e). Aitken mode (20 – 80 nm) particle concentrations are variable between years (maximum mode at 260 cm$^{-3}$ and minimum mode at 100 cm$^{-3}$). Coarse mode (> 1 μm) concentrations are below 10 cm$^{-3}$, while nucleation mode (< 20 nm) concentrations are commonly below 100 cm$^{-3}$ (Fig. 1h,j). Correlation analysis of all data shows that CCN concentration correlates well with $N_{tot}$ (R= 0.76) as well as accumulation (R=0.85) and Aitken (R= 0.60) mode particle number concentrations (Fig. S3). This suggests that the availability of aerosol particles, especially accumulation mode particles, is an important driver behind CCN concentration over the GBR.

Kappa values, calculated for those datasets in which multiple CCN supersaturation measurements and size distribution measurements were available, exhibit significant variability between datasets (Fig. 1j). In particular, December 2021 dataset exhibits kappa values that are often larger than 0.7 (Fig. 1j) but with large variability, suggesting significant inorganic fraction (Petters and Kreidenweis, 2007) in the aerosol particles as well as complex sources. The 2023 measurements on the other hand, show kappa values largely below 0.2 (Fig. 1j), suggesting mostly organic particles (Petters and Kreidenweis, 2007). This can likely be explained by the 2023 measurements being the only ones taking place directly on a coral cay instead of on a ship. Therefore, local biogenic sources will contribute to growth of particles and result in more organic particle composition.

https://doi.org/10.5194/ar-2026-9
Preprint. Discussion started: 16 February 2026


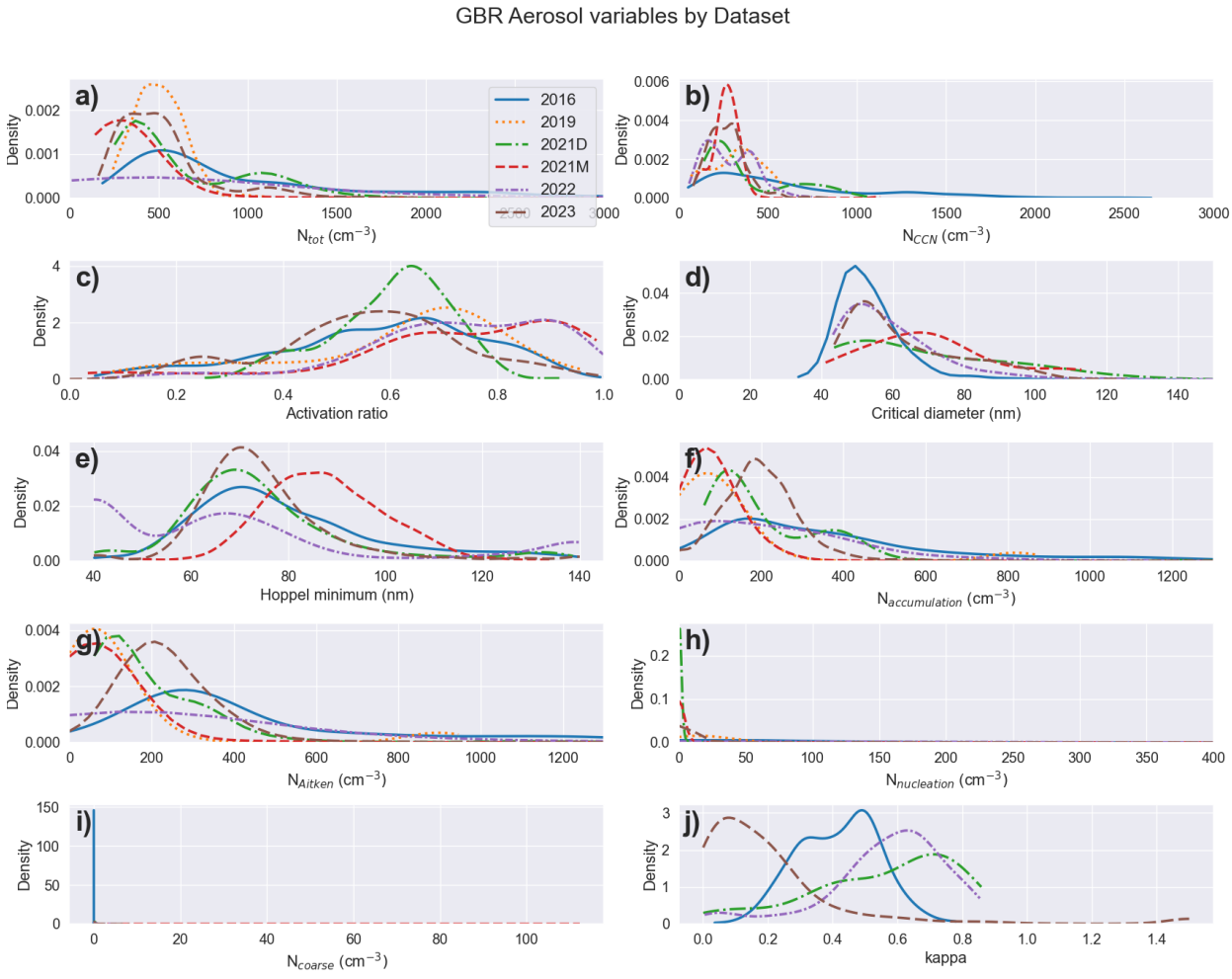


Figure 1: Kernel density estimates for in-situ aerosol-related variables collected at the GBR or calculated from them during spring (blue) and summer (orange). The variables shown are, total particle (a) and CCN (b) number concentration, CCN activation ratio (c), critical diameter (d), Hoppel minimum (e), accumulation (f), Aitken (g), nucleation (h), and coarse (i) mode number concentration and kappa parameter (j).

### 3.2 Spatiotemporal variability of CCN and aerosols over GBR

The CCN concentrations do not reveal any monotonal spatial trend, however, the spatial distribution of observed CCN concentration is visually comparable to the spatial distribution of measured $N_{tot}$ (Fig. S4). The varying speed and scale of aerosol processes (from growth and evaporation in seconds to synoptic scale processes taking days), and the non-continuous spatially heterogeneous measurements make detecting spatial variability in our dataset very difficult.

https://doi.org/10.5194/ar-2026-9
Preprint. Discussion started: 16 February 2026



In terms of temporal variance, the highest median $N_{tot}$ and CCN concentrations are observed during the 2016 measurements. The 2016 CCN concentrations are statistically different from the 2023 measurements, but otherwise concentrations are similar campaign-to-campaign (Fig. 2a). The CCN activation ratio, remains stable independent of the campaigns with no statistically significant differences between campaigns (Fig. 2b). Total particle number concentration splits into three groups, with 2016 and 2019 being statistically similar, measurements post December 2021 inclusive being similar with one another, and the low concentrations measured during the March 2021 campaign standing out from the rest (Fig. 2c). Any temporal effects may be confounded by spatial effects caused by uneven spatial coverage across the dataset. However, even limiting the dataset to just central and southern GBR and avoiding the sparser northern GBR, the temporal effects appear similar (Fig. S5).

### 3.3 Cloud processing

Cloud processing occurs to particles with diameters large enough to activate as CCN (Seinfeld and Pandis, 2016). In air masses where cloud processing has occurred, particularly marine air masses, this can usually be identified by the presence of a Hoppel minimum (Hoppel et al., 1985). Our analysis shows that over the GBR, a Hoppel minimum is observed in the size distribution in 92% of times, suggesting that cloud processing commonly occurs in the air masses that reach the reef (Braga et al., 2025). To investigate processes affecting CCN concentrations and hence cloud processing over the GBR, several parameters were compared, binned by the CCN concentration (Fig. S6).

https://doi.org/10.5194/ar-2026-9
Preprint. Discussion started: 16 February 2026


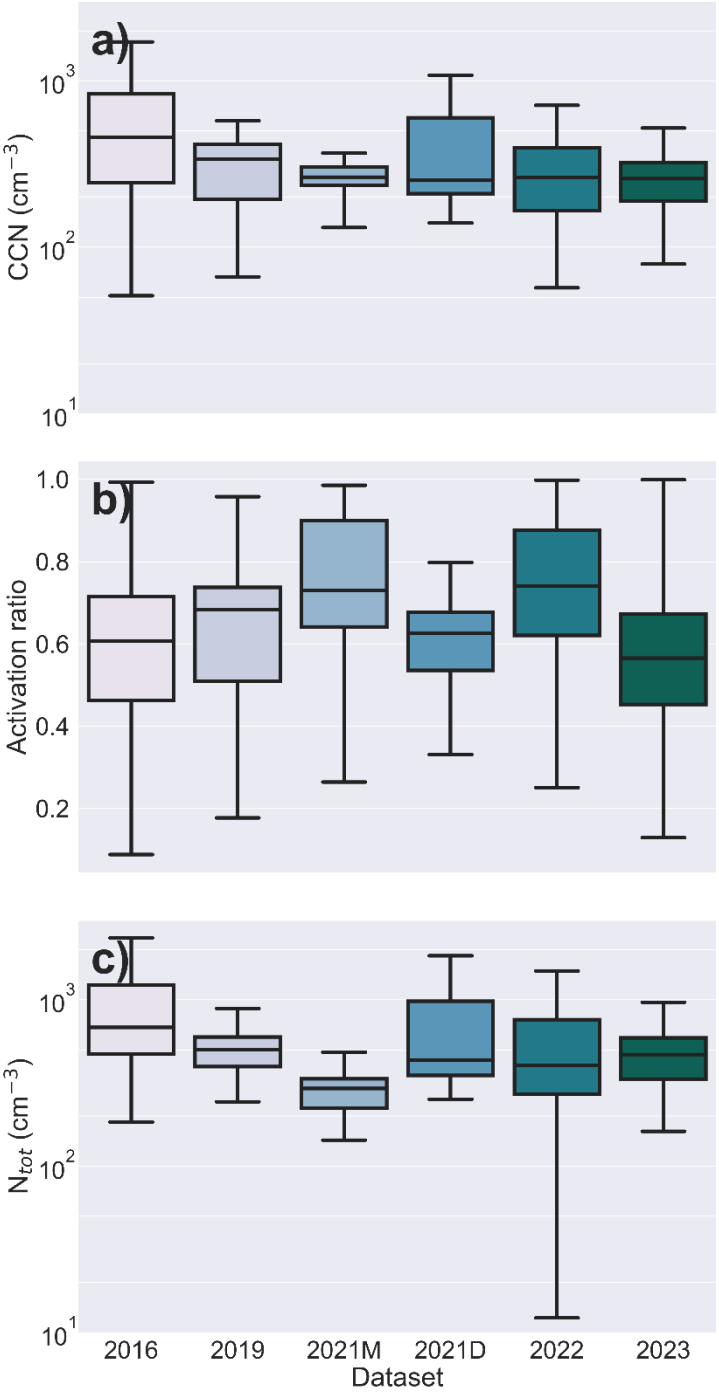


Figure 2: Temporal variability of CCN concentration (at 0.5% SS) (a), activation ratio (b), and $N_{tot}$ (c). The middle line of a boxplot represents the median value, the upper and lower edges of a box show the interquartile range, and the whiskers show the entire range. 2021M and 2021D mean 2021 March and 2021 December, respectively.

https://doi.org/10.5194/ar-2026-9
Preprint. Discussion started: 16 February 2026


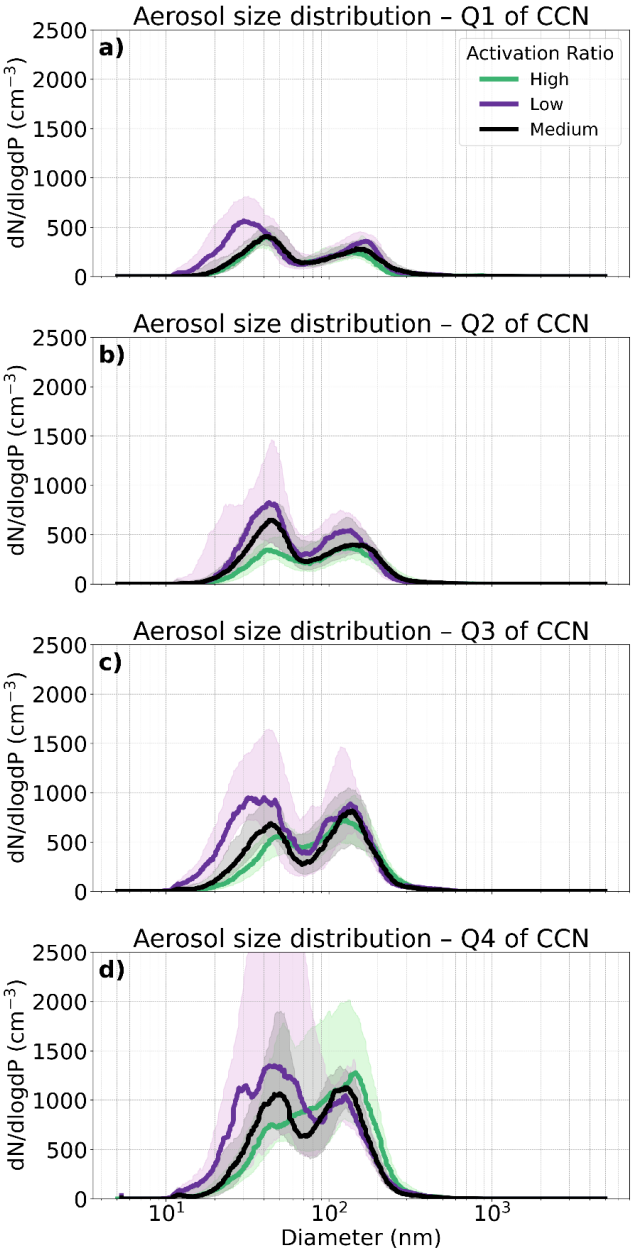


Figure 3: Aerosol size distributions for the four quartiles of CCN concentrations (a, b, c, d). Aerosol size distributions are coloured by the relative values of activation ratio (Low – purple, Medium – black, High– green). Shaded areas present the interquartile ranges. Values of activation ratio ranges for each CCN concentration quartile as well as values of CCN concentration quartile are listed in Table S2.

CCN concentration appears to increase with both $N_{tot}$ and activation ratio, but the activation ratio begins to plateau at around 0.7 for CCN concentrations higher than 340 cm$^{-3}$ (Fig. S6). During times when the CCN concentrations are below the median

https://doi.org/10.5194/ar-2026-9
Preprint. Discussion started: 16 February 2026




(Q1 and Q2), the size distribution remains stable for medium and high activation ratios, while low activation ratios are generally associated with a smaller Aitken mode diameter and an enriched Aitken mode concentration (Fig. 3a, b). At higher CCN concentrations, the Aitken mode peak widens considerably towards smaller sizes, suggesting an influx of ultrafine particles, possibly from local sources (Fig. 3c, d). At the fourth quartile (Q4) CCN concentration, a separate nucleation mode peak is observed during low activation ratio periods, further suggesting influence from more local sources. At high activation ratios, the Hoppel minimum disappears, suggesting transport of air masses that have not undergone recent cloud processing (Fig. 3). Considering the high concentrations of accumulation mode particles and small fraction of Aitken mode particles, it is likely this is due to non-marine sources from the Australian continent. These periods match with the highest CCN concentrations as observed in Figure S6, where extreme CCN concentrations are associated with an increase in land fraction, the fraction of time the air mass spent over the continent. Overall, these findings suggest there could be two mechanisms that contributed to increased CCN concentrations over the reef, continental transport or locally created new particles.

### 3.4 Plausible drivers of atmospheric CCN concentration

To estimate the importance of atmospheric variables to CCN concentrations over the reef, a gradient-boosting regression model was constructed. The dataset (n = 1944) was split into 80/20 into a training and a test set. Features that showed a statistically significant change in the feature importance analysis are showed in Fig. 4 while the full table of inputs can be found in Fig. S7. The model performs very well for the test set ($r^2 = 0.907$).

The analysis shows that accumulation mode particle number concentration is the strongest predictor of CCN concentration, with higher accumulation mode concentration leading to higher CCN concentration (Fig. S8 a,b). Aitken mode concentration is the second-best predictor. Critical diameter and sea surface temperature appear to play a role as well, with higher critical diameter reducing CCN concentration and sea surface temperature extremes increasing CCN concentration. Finally, black carbon concentration, nucleation mode concentration and activation ratio appear to have a small but statistically significant effect. The above results suggest that while accumulation mode concentration primarily drives CCN concentration, smaller particles in the sub-100 nm range have an effect. However, nucleation mode concentrations are considered underestimated as they are subject to notable uncertainties in charging and detection efficiency (Kangasluoma et al., 2020), and thus some nucleation mode dynamics are underrepresented. Nucleation mode particles will also not directly contribute to CCN concentration due to being too small to be activated as CCN. However, they can still contribute indirectly by first growing to larger sizes or by coagulating and contributing to the size of larger particles.

The effect of Aitken mode particles on CCN concentration was investigated by counterfactual modelling approach using the gradient boosting algorithm (see Methods section). This method was chosen because a simple subtraction of accumulation mode concentration from CCN concentration might not capture the complicated aerosol dynamics present in the ambient atmosphere and might over or underestimate the true effect of Aitken mode particles to CCN. For example, a smaller Aitken mode concentration would likely affect coagulation scavenging to accumulation mode. A modelling approach allows keeping the inherent relationships of the ambient variables intact while minimizing Aitken mode concentration in a believable way.

https://doi.org/10.5194/ar-2026-9
Preprint. Discussion started: 16 February 2026


The results show that Aitken mode particle concentration can contribute 5.6 % (4.6 % - 5.9 % confidence intervals) to CCN concentration over the GBR (Fig. S9). The contribution is calculated from counterfactual modelling with confidence intervals representing the 5$^{th}$ and 95$^{th}$ percentiles of the effect from bootstrapping.

To examine whether the Aitken mode is sensitive to specific sources or geographic regions, we examine the air mass back trajectories that coincided with the highest and lowest quartiles of aerosol number fraction contributed by the Aitken mode. A shorter 6-hour back trajectory was selected to this analysis. This was done for several reasons. The GBR reef lagoon is geographically limited, and therefore longer back-trajectories could mask the effect of time spent over the reef lagoon. The processing of ultrafine particles also occurs typically within a few hours, and therefore longer back trajectories would not add significant information regarding local source contribution. Therefore, this shorter back trajectory should improve the interpretability of the results and better capture actual local source contributions. Figure 5a-d represents two geographic areas where our dataset contains a high density of data points in a small area, 0.5° x 0.5° or approx. 55 x 55 km each. When Aitken mode enrichment occurs, air masses predominantly travel over the reef rather than the open ocean. This is also a general trend, in which increased time spent over the reef enriches the Aitken mode in both the Central and Southern GBR irrespective of whether we are measuring on a reef or on open ocean (Fig. 5g). These air masses also typically travel at lower altitudes and always within the mixing layer during periods of Aitken mode enrichment, increasing exposure to surface fluxes (Fig. 5 e-f).

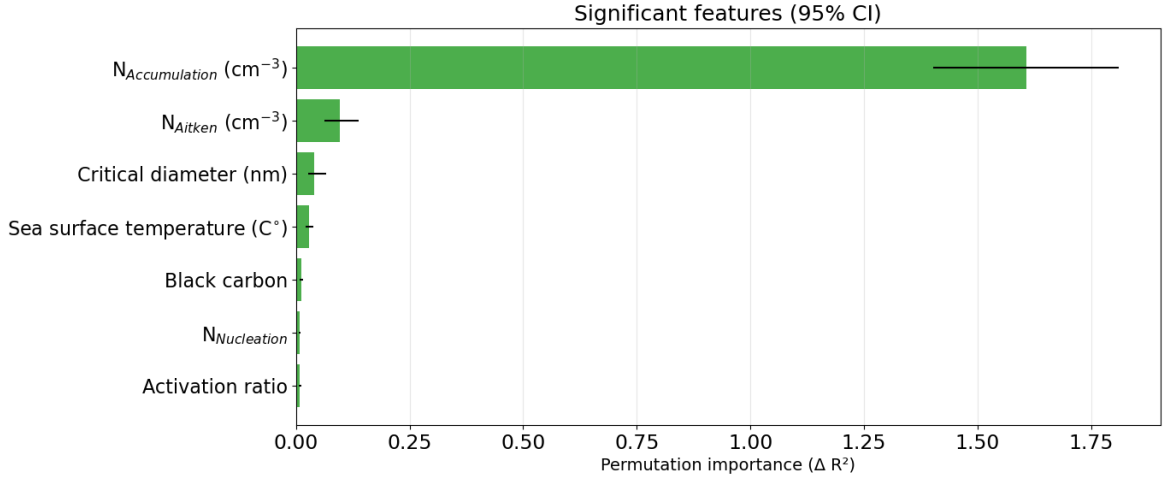


Figure 4: Permutation feature importance of climate variables in explaining CCN concentration. The differences between original and permuted mean square errors on the x-axis indicate how important each feature is in predicting the CCN concentration, with larger difference between original and permuted values indicating a more important feature. The black whiskers indicate 95% confidence intervals. The number of permutations used was 10000.

https://doi.org/10.5194/ar-2026-9
Preprint. Discussion started: 16 February 2026


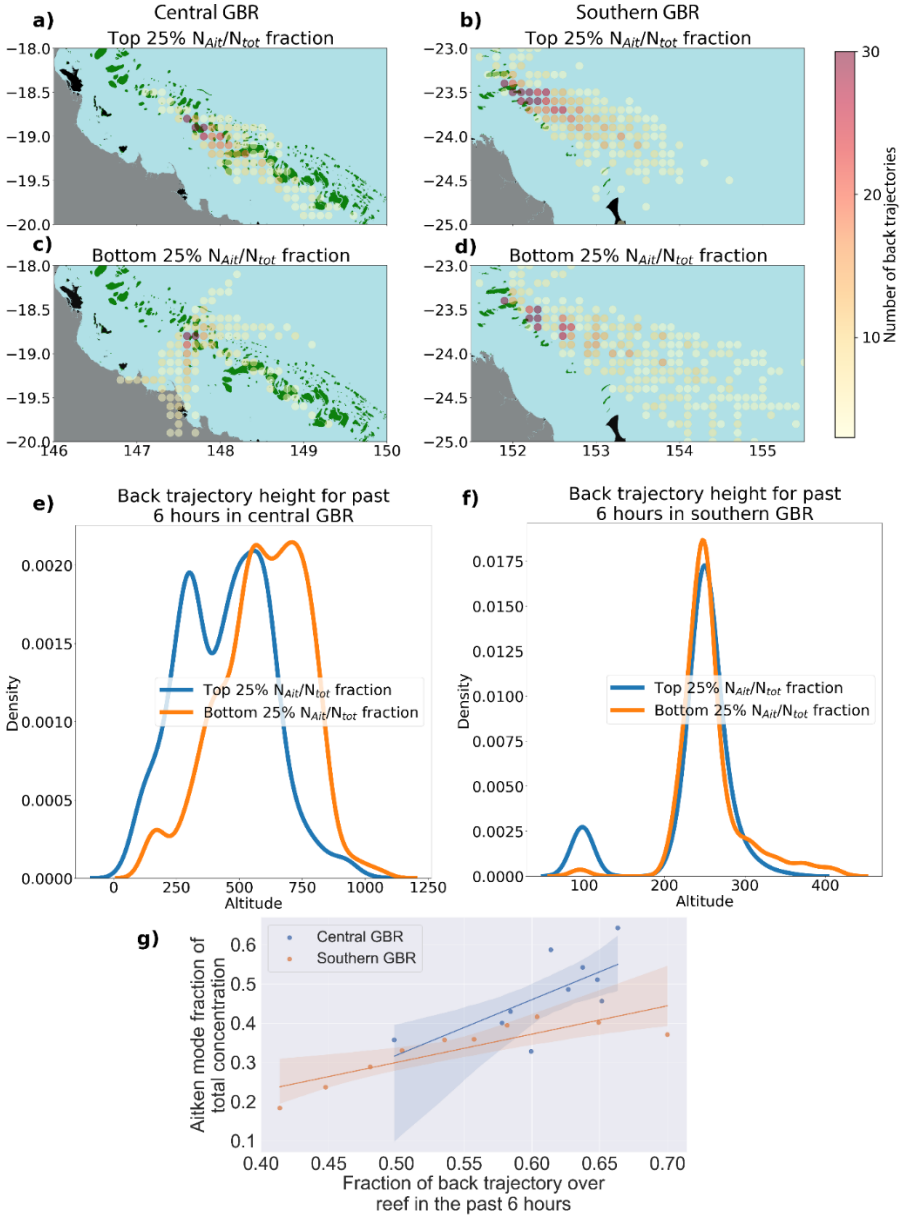


Figure 5: Spatial distribution of 6-hour back trajectories for data with top 25-percentile (a, b) and bottom 25-percentile (c,d) of Aitken mode fraction in proportion to total particle concentration in Central GBR (left) and Southern GBR (right). Kernel density estimates for the back trajectory altitude for top 25% (blue) and bottom 25% (orange) Aitken mode fraction in central (e) and southern (f) GBR. Fraction of the total aerosol number concentration in the Aitken mode plotted against the proportion of the past six hours during which the air mass was over the reef at Central and Southern GBR (g). The lines are linear fits to calculated Aitken mode fraction quantiles and their respective reef fractions. Shaded areas represent the line fit uncertainty.

https://doi.org/10.5194/ar-2026-9
Preprint. Discussion started: 16 February 2026




## 4 Conclusions

Aerosol concentrations over the GBR are typical of a clean coastal environment (Dall'Osto et al., 2011) sitting somewhere between a clean marine (Humphries et al., 2021, 2023) and Australian land environment (Chen et al., 2019; Milic et al., 2017; Tessendorf et al., 2013). The observed air masses frequently went through cloud processing resulting in a particle number size distribution that often contains a Hoppel minimum (92%). While mode values of most particle parameters, $N_{tot}$, CCN concentration, accumulation mode particle concentration, and Hoppel minimum, are comparable between most measurements, the hygroscopicity parameter exhibits significant variability between data. This suggests that a variety of different aerosol particles were captured in terms of chemical composition. The heavily organic particles measured at Heron Island in 2023 are of particular note, as the stark difference suggests local organic emissions could play a key role in aerosol loading over coral cays and islands.

As it stands, it appears that the magnitude of aerosol loading over the GBR is primarily influenced by long-range transport of aerosol particles. It is also apparent that there is a non-negligible effect from local sources. Air masses traveling over the reef are enriched in small particles, and their local contribution to CCN concentration is up to 6% (Fig. S9). Meteorology, sea surface temperature in particular, appears to play a role as well. However, although meteorological conditions do vary over the reef, their effect on CCN concentration is notably small. It could be that the meteorological effect is contained in the changing aerosol loading and the residual effect in our statistical modelling is small. We can hypothesize that long-term changes in climate and weather patterns such as ENSO and Southern Oscillation will affect CCN concentrations but primarily by affecting aerosol sources and sinks as well as vertical mixing due to changes in the sea surface temperature and boundary layer height. However, confirming this hypothesis requires consistent long-term measurements over the GBR, preferably in consistent multiple stationary locations.

While likely negligible at global scales, the reef signal detected in this study represents a unique natural marine source that can influence regional CCN budgets and cloud microphysics. It is important to note that we cannot distinguish between various sources within the coral reef ecosystem, and therefore quantifying the exact sources within the ecosystem itself remains a subject of future work. Furthermore, this analysis method could be extended to cover other biologically active systems that are potentially important regional sources of CCN.

Coral reef contributions to aerosols and CCN are typically not explicitly parameterized in climate models. This analysis highlights the importance of resolving atmosphere-biosphere processes at fine spatial scales to capture subtle but climatically relevant sources of CCN. By directly isolating and quantifying the effect of coral reef emissions on CCN concentrations, our study provides, to our knowledge, the first direct observational evidence of a reef-origin aerosol contribution to cloud-relevant particle populations using ambient in situ measurements. Our results offer a novel constraint for regional modelling and a foundation for incorporating biogenic aerosol processes from reef systems into Earth system models.

https://doi.org/10.5194/ar-2026-9
Preprint. Discussion started: 16 February 2026




## Code and data availability

The dataset used this in study is available in https://figshare.com/articles/dataset/Coral_reef_emissions_enhance_aerosol_and_cloud_condensation_nuclei_concentrations_over_the_Great_Barrier_Reef/30193285?file=58177546 or upon request from the corresponding author by email.

## Author Contributions

J.S. and M.O. wrote the manuscript, analyzed the data and prepared the figures. J.A., Z.L., E.J.H., L.C., B.M., D.H. and L.H. collected the data, J.S., M.O., J.A., Z.L. and E.J.H. processed the data. B.M, D.H. and Z.R. conceptualized the study. All co-authors provided comments and reviewed the manuscript.

## Acknowledgement

The authors would like to acknowledge the Traditional Owners of the Great Barrier Reef, particularly the groups from the PCCC TUMRA for permission to collect atmospheric aerosol data in/on their sea Country.

## Financial Support

This research was funded by the Reef Restoration and Adaptation Program through the partnership between the Australian Governments Reef Trust and the Great Barrier Reef Foundation and supported by a grant of sea time on RV Investigator from the CSIRO Marine National Facility (https://ror.org/01mae9353).

## References

Adler, A. I. and Painsky, A.: Feature Importance in Gradient Boosting Trees with Cross-Validation Feature Selection, Entropy, 24, 687, https://doi.org/10.3390/e24050687, 2022.

Coral bleaching events | AIMS: https://www.aims.gov.au/research-topics/environmental-issues/coral-bleaching/coral-bleaching-events, last access: 10 February 2025.

Ansmann, A., Ohneiser, K., Engelmann, R., Radenz, M., Griesche, H., Hofer, J., Althausen, D., Creamean, J. M., Boyer, M. C., Knopf, D. A., Dahlke, S., Maturilli, M., Gebauer, H., Bühl, J., Jimenez, C., Seifert, P., and Wandinger, U.: Annual cycle of aerosol properties over the central Arctic during MOSAiC 2019–2020 – light-extinction, CCN, and INP levels from the boundary layer to the tropopause, Atmospheric Chem. Phys., 23, 12821–12849, https://doi.org/10.5194/acp-23-12821-2023, 2023.

Berkelmans, R.: Time-integrated thermal bleaching thresholds of reefs and their variation on the Great Barrier Reef, Mar. Ecol. Prog. Ser., 229, 73–82, https://doi.org/10.3354/meps229073, 2002.

https://doi.org/10.5194/ar-2026-9
Preprint. Discussion started: 16 February 2026


Braga, R. C., Rosenfeld, D., Hernandez, D., Medcraft, C., Efraim, A., Moser, M., Lucke, J., Doss, A., and Harrison, D.: Cloud processing dominates the vertical profiles of aerosols in marine air masses over the Great Barrier Reef, Atmospheric Res., 315, 107928, https://doi.org/10.1016/j.atmosres.2025.107928, 2025.

Breiman, L.: Random Forests, Mach. Learn., 45, 5–32, https://doi.org/10.1023/A:1010933404324, 2001.

Brown, B. E.: Coral bleaching: causes and consequences, Coral Reefs, 16, S129–S138, https://doi.org/10.1007/s003380050249, 1997.

Chen, Z., Schofield, R., Rayner, P., Zhang, T., Liu, C., Vincent, C., Fiddes, S., Ryan, R. G., Alroe, J., Ristovski, Z. D., Humphries, R. S., Keywood, M. D., Ward, J., Paton-Walsh, C., Naylor, T., and Shu, X.: Characterization of aerosols over the Great Barrier Reef: The influence of transported continental sources, Sci. Total Environ., 690, 426–437, https://doi.org/10.1016/j.scitotenv.2019.07.007, 2019.

Coddington, O., Lean, J. L., Pilewskie, P., Snow, M., and Lindholm, D.: A Solar Irradiance Climate Data Record, Bull. Am. Meteorol. Soc., 97, 1265–1282, https://doi.org/10.1175/BAMS-D-14-00265.1, 2016.

Courtial, L., Roberty, S., Shick, J. M., Houlbrèque, F., and Ferrier-Pagès, C.: Interactive effects of ultraviolet radiation and thermal stress on two reef-building corals, Limnol. Oceanogr., 62, 1000–1013, https://doi.org/10.1002/lno.10481, 2017.

Cropp, R., Gabric, A., van Tran, D., Jones, G., Swan, H., and Butler, H.: Coral reef aerosol emissions in response to irradiance stress in the Great Barrier Reef, Australia, Ambio, 47, 671–681, https://doi.org/10.1007/s13280-018-1018-y, 2018.

Dall'Osto, M., Monahan, C., Greaney, R., Beddows, D. C. S., Harrison, R. M., Ceburnis, D., and O'Dowd, C. D.: A statistical analysis of North East Atlantic (submicron) aerosol size distributions, Atmospheric Chem. Phys., 11, 12567–12578, https://doi.org/10.5194/acp-11-12567-2011, 2011.

Deschaseaux, E. S. M., Dunne, E., Schulz, K. G., Eyre, B. D., and Harrison, D. P.: The Central Great Barrier Reef as a Net Source of Climatically Relevant Biogenic Volatile Organic Compounds, J. Geophys. Res. Oceans, 130, e2024JC021192, https://doi.org/10.1029/2024JC021192, 2025.

Dietzel, A., Bode, M., Connolly, S. R., and Hughes, T. P.: The population sizes and global extinction risk of reef-building coral species at biogeographic scales, Nat. Ecol. Evol., 5, 663–669, https://doi.org/10.1038/s41559-021-01393-4, 2021.

Doshi-Velez, F. and Kim, B.: Towards A Rigorous Science of Interpretable Machine Learning, https://doi.org/10.48550/arXiv.1702.08608, 2 March 2017.

Eckert, C., Monteforte, K. I., Harrison, D. P., and Kelaher, B. P.: Exploring Meteorological Conditions and Microscale Temperature Inversions above the Great Barrier Reef through Drone-Based Measurements, Drones, 7, 695, https://doi.org/10.3390/drones7120695, 2023.

Eckert, C., Hernandez-Jaramillo, D. C., Medcraft, C., Harrison, D. P., and Kelaher, B. P.: Drone-Based Measurement of the Size Distribution and Concentration of Marine Aerosols above the Great Barrier Reef, Drones, 8, 292, https://doi.org/10.3390/drones8070292, 2024.

Fiddes, S. L., Woodhouse, M. T., Utembe, S., Schofield, R., Alexander, S. P., Alroe, J., Chambers, S. D., Chen, Z., Cravigan, L., Dunne, E., Humphries, R. S., Johnson, G., Keywood, M. D., Lane, T. P., Miljevic, B., Omori, Y., Protat, A., Ristovski, Z.,

https://doi.org/10.5194/ar-2026-9
Preprint. Discussion started: 16 February 2026


Selleck, P., Swan, H. B., Tanimoto, H., Ward, J. P., and Williams, A. G.: The contribution of coral-reef-derived dimethyl sulfide to aerosol burden over the Great Barrier Reef: a modelling study, Atmospheric Chem. Phys., 22, 2419–2445, https://doi.org/10.5194/acp-22-2419-2022, 2022.

Fox-Kemper, B., Hewitt, H. T., Xiao, C., Aðalgeirsdóttir, G., Drijfhout, S. S., Edwards, T. L., Golledge, N. R., Hemer, M., Kopp, R., Krinner, G., Mix, A., Notz, D., Nowicki, S., Nurhati, I. S., Ruiz, L., Sallée, J.-B., Slangen, A. B. A., and Yu, Y.: Ocean, Cryosphere and Sea Level Change, in: Climate Change 2021: The Physical Science Basis. Contribution of Working Group I to the Sixth Assessment Report of the Intergovernmental Panel on Climate Change, edited by: Masson-Delmotte, V., Zhai, P., Pirani, S. L., Connors, S. L., Péan, C., Berger, S., Caud, Y., Chen, L., Goldfarb, L., Gomis, M. I., Huang, M., Leitzell, K., Lonnoy, E., Matthews, J. B. R., Maycock, T. K., Waterfield, T., Yelekçi, O., Yu, R., and Zhou, B., Cambridge University Press, Cambridge, United Kingdom and New York, NY, USA, 1211–1362, https://doi.org/10.1017/9781009157896.011, 2021.

Friedman, J. H.: Greedy function approximation: A gradient boosting machine., Ann. Stat., 29, 1189–1232, https://doi.org/10.1214/aos/1013203451, 2001.

Great Barrier Reef Marine Park Authority: Great Barrier Reef (GBR) Features, 2007.

Harris, D. L., Rovere, A., Casella, E., Power, H., Canavesio, R., Collin, A., Pomeroy, A., Webster, J. M., and Parravicini, V.: Coral reef structural complexity provides important coastal protection from waves under rising sea levels, Sci. Adv., 4, eaao4350, https://doi.org/10.1126/sciadv.aao4350, 2018.

Harrison, D. P.: An Overview of Environmental Engineering Methods for Reducing Coral Bleaching Stress, in: Oceanographic Processes of Coral Reefs, CRC Press, 2024.

Hernandez-Jaramillo, D. C., Medcraft, C., Braga, R. C., Butcherine, P., Doss, A., Kelaher, B., Rosenfeld, D., and Harrison, D. P.: New airborne research facility observes sensitivity of cumulus cloud microphysical properties to aerosol regime over the great barrier reef, Environ. Sci. Atmospheres, 4, 861–871, https://doi.org/10.1039/D4EA00009A, 2024.

Hernandez-Jaramillo, D. C., Harrison, L., Gunner, G., McGrath, A., Junkermann, W., Lieff, W., Hacker, J., Rosenfeld, D., Kelaher, B., and Harrison, D. P.: First generation outdoor marine cloud brightening trial increases aerosol concentration at cloud base height, Environ. Res. Lett., 20, 054065, https://doi.org/10.1088/1748-9326/adccd7, 2025.

Hersbach, H., Bell, B., Berrisford, P., Biavati, G., Horányi, A., Muñoz Sabater, J., Nicolas, J., Peubey, C., Radu, R., Schepers, D., Simmons, A., Soci, C., Dee, D., and Thépaut, J.-N.: ERA5 hourly data on single levels from 1940 to present., https://doi.org/10.24381/cds.adbb2d47, 2023.

Hoppel, W. A., Fitzgerald, J. W., and Larson, R. E.: Aerosol size distributions in air masses advecting off the east coast of the United States, J. Geophys. Res. Atmospheres, 90, 2365–2379, https://doi.org/10.1029/JD090iD01p02365, 1985.

Horchler, E. J., Alroe, J., Harrison, L., Cravigan, L., Harrison, D. P., and Ristovski, Z. D.: Measurement report: Aerosol and cloud nuclei properties along the Central and Northern Great Barrier Reef: Impact of continental emissions , EGUsphere, 1–21, https://doi.org/10.5194/egusphere-2025-465, 2025.

https://doi.org/10.5194/ar-2026-9
Preprint. Discussion started: 16 February 2026


Hughes, T. P., Barnes, M. L., Bellwood, D. R., Cinner, J. E., Cumming, G. S., Jackson, J. B. C., Kleypas, J., van de Leemput, I. A., Lough, J. M., Morrison, T. H., Palumbi, S. R., van Nes, E. H., and Scheffer, M.: Coral reefs in the Anthropocene, Nature, 546, 82–90, https://doi.org/10.1038/nature22901, 2017a.

Hughes, T. P., Kerry, J. T., Álvarez-Noriega, M., Álvarez-Romero, J. G., Anderson, K. D., Baird, A. H., Babcock, R. C., Beger, M., Bellwood, D. R., Berkelmans, R., Bridge, T. C., Butler, I. R., Byrne, M., Cantin, N. E., Comeau, S., Connolly, S. R., Cumming, G. S., Dalton, S. J., Diaz-Pulido, G., Eakin, C. M., Figueira, W. F., Gilmour, J. P., Harrison, H. B., Heron, S. F., Hoey, A. S., Hobbs, J.-P. A., Hoogenboom, M. O., Kennedy, E. V., Kuo, C., Lough, J. M., Lowe, R. J., Liu, G., McCulloch, M. T., Malcolm, H. A., McWilliam, M. J., Pandolfi, J. M., Pears, R. J., Pratchett, M. S., Schoepf, V., Simpson, T., Skirving, W. J., Sommer, B., Torda, G., Wachenfeld, D. R., Willis, B. L., and Wilson, S. K.: Global warming and recurrent mass bleaching of corals, Nature, 543, 373–377, https://doi.org/10.1038/nature21707, 2017b.

Humphries, R. S., McRobert, I. M., Ponsonby, W. A., Ward, J. P., Keywood, M. D., Loh, Z. M., Krummel, P. B., and Harnwell, J.: Identification of platform exhaust on the RV Investigator, Atmospheric Meas. Tech., 12, 3019–3038, https://doi.org/10.5194/amt-12-3019-2019, 2019.

Humphries, R. S., Keywood, M. D., Gribben, S., McRobert, I. M., Ward, J. P., Selleck, P., Taylor, S., Harnwell, J., Flynn, C., Kulkarni, G. R., Mace, G. G., Protat, A., Alexander, S. P., and McFarquhar, G.: Southern Ocean latitudinal gradients of cloud condensation nuclei, Atmospheric Chem. Phys., 21, 12757–12782, https://doi.org/10.5194/acp-21-12757-2021, 2021.

Humphries, R. S., Keywood, M. D., Ward, J. P., Harnwell, J., Alexander, S. P., Klekociuk, A. R., Hara, K., McRobert, I. M., Protat, A., Alroe, J., Cravigan, L. T., Miljevic, B., Ristovski, Z. D., Schofield, R., Wilson, S. R., Flynn, C. J., Kulkarni, G. R., Mace, G. G., McFarquhar, G. M., Chambers, S. D., Williams, A. G., and Griffiths, A. D.: Measurement report: Understanding the seasonal cycle of Southern Ocean aerosols, Atmospheric Chem. Phys., 23, 3749–3777, https://doi.org/10.5194/acp-23-3749-2023, 2023.

Jackson, R., Gabric, A., and Cropp, R.: Effects of ocean warming and coral bleaching on aerosol emissions in the Great Barrier Reef, Australia, Sci. Rep., 8, 14048, https://doi.org/10.1038/s41598-018-32470-7, 2018.

Kangasluoma, J., Cai, R., Jiang, J., Deng, C., Stolzenburg, D., Ahonen, L. R., Chan, T., Fu, Y., Kim, C., Laurila, T. M., Zhou, Y., Dada, L., Sulo, J., Flagan, R. C., Kulmala, M., Petäjä, T., and Lehtipalo, K.: Overview of measurements and current instrumentation for 1–10 nm aerosol particle number size distributions, J. Aerosol Sci., 148, 105584, https://doi.org/10.1016/j.jaerosci.2020.105584, 2020.

Knowlton, N., Brainard, R. E., Fisher, R., Moews, M., Plaisance, L., and Caley, M. J.: Coral Reef Biodiversity, in: Life in the World's Oceans, John Wiley & Sons, Ltd, 65–78, https://doi.org/10.1002/9781444325508.ch4, 2010.

Krüger, M. L., Mertes, S., Klimach, T., Cheng, Y. F., Su, H., Schneider, J., Andreae, M. O., Pöschl, U., and Rose, D.: Assessment of cloud supersaturation by size-resolved aerosol particle and cloud condensation nuclei (CCN) measurements, Atmospheric Meas. Tech., 7, 2615–2629, https://doi.org/10.5194/amt-7-2615-2014, 2014.

https://doi.org/10.5194/ar-2026-9
Preprint. Discussion started: 16 February 2026


Laing, J. R., Jaffe, D. A., and Arthur J. Sedlacek, I. I. I.: Comparison of Filter-based Absorption Measurements of Biomass Burning Aerosol and Background Aerosol at the Mt. Bachelor Observatory, Aerosol Air Qual. Res., 20, 663–678, https://doi.org/10.4209/aaqr.2019.06.0298, 2020.

Law, C. S., Smith, M. J., Harvey, M. J., Bell, T. G., Cravigan, L. T., Elliott, F. C., Lawson, S. J., Lizotte, M., Marriner, A., McGregor, J., Ristovski, Z., Safi, K. A., Saltzman, E. S., Vaattovaara, P., and Walker, C. F.: Overview and preliminary results of the Surface Ocean Aerosol Production (SOAP) campaign, Atmospheric Chem. Phys., 17, 13645–13667, https://doi.org/10.5194/acp-17-13645-2017, 2017.

Li, Z., Harrison, L., Alroe, J., Scoble, H., Chen, C., Medcraft, C., Holloway, C., Brown, R., Baker, P., Harrison, D. P., and Ristovski, Z.: Characterizing the Crosswind Structure of Artificial Seawater Droplet Plumes during a Sea Trial on the Great Barrier Reef, Environ. Sci. Technol., 59, 27222–27229, https://doi.org/10.1021/acs.est.5c10024, 2025.

Lundberg, S. M. and Lee, S.-I.: A Unified Approach to Interpreting Model Predictions, in: Advances in Neural Information Processing Systems, 2017.

Manshausen, P., Watson-Parris, D., Christensen, M. W., Jalkanen, J.-P., and Stier, P.: Invisible ship tracks show large cloud sensitivity to aerosol, Nature, 610, 101–106, https://doi.org/10.1038/s41586-022-05122-0, 2022.

Marelle, L., Myhre, G., Thomas, J. L., and Raut, J.-C.: Aerosol Background Concentrations Influence Aerosol-Cloud Interactions as Much as the Choice of Aerosol-Cloud Parameterization, Geophys. Res. Lett., 52, e2024GL111780, https://doi.org/10.1029/2024GL111780, 2025.

Milic, A., Mallet, M. D., Cravigan, L. T., Alroe, J., Ristovski, Z. D., Selleck, P., Lawson, S. J., Ward, J., Desservettaz, M. J., Paton-Walsh, C., Williams, L. R., Keywood, M. D., and Miljevic, B.: Biomass burning and biogenic aerosols in northern Australia during the SAFIRED campaign, Atmospheric Chem. Phys., 17, 3945–3961, https://doi.org/10.5194/acp-17-3945-2017, 2017.

Modini, R. L., Ristovski, Z. D., Johnson, G. R., He, C., Surawski, N., Morawska, L., Suni, T., and Kulmala, M.: New particle formation and growth at a remote, sub-tropical coastal location, Atmospheric Chem. Phys., 9, 7607–7621, https://doi.org/10.5194/acp-9-7607-2009, 2009.

Noble, S. R. and Hudson, J. G.: Effects of Continental Clouds on Surface Aitken and Accumulation Modes, J. Geophys. Res. Atmospheres, 124, 5479–5502, https://doi.org/10.1029/2019JD030297, 2019.

Pedregosa, F., Varoquaux, G., Gramfort, A., Michel, V., Thirion, B., Grisel, O., Blondel, M., Prettenhofer, P., Weiss, R., Dubourg, V., Vanderplas, J., Passos, A., Cournapeau, D., Brucher, M., Perrot, M., and Duchesnay, É.: Scikit-learn: Machine Learning in Python, J. Mach. Learn. Res., 12, 2825–2830, 2011.

Peltola, M., Rose, C., Trueblood, J. V., Gray, S., Harvey, M., and Sellegri, K.: New particle formation in coastal New Zealand with a focus on open-ocean air masses, Atmospheric Chem. Phys., 22, 6231–6254, https://doi.org/10.5194/acp-22-6231-2022, 2022.

Petters, M. D. and Kreidenweis, S. M.: A single parameter representation of hygroscopic growth and cloud condensation nucleus activity, Atmospheric Chem. Phys., 7, 1961–1971, https://doi.org/10.5194/acp-7-1961-2007, 2007.

https://doi.org/10.5194/ar-2026-9
Preprint. Discussion started: 16 February 2026


Reaka, M.: The global biodiversity of coral reefs: a comparison with rainforests, 1997.

Richards, L. S., Siems, S. T., Huang, Y., Zhao, W., Harrison, D. P., Manton, M. J., and Reeder, M. J.: The meteorological drivers of mass coral bleaching on the central Great Barrier Reef during the 2022 La Niña, Sci. Rep., 14, 23867, https://doi.org/10.1038/s41598-024-74181-2, 2024.

Riemer, N., Ault, A. P., West, M., Craig, R. L., and Curtis, J. H.: Aerosol Mixing State: Measurements, Modeling, and Impacts, Rev. Geophys., 57, 187–249, https://doi.org/10.1029/2018RG000615, 2019.

Rowland, M. J., Lambrides ,Ariana B. J., McNiven ,Ian J., and and Ulm, S.: Great Barrier Reef Indigenous archaeology and occupation of associated reef and continental islands, Australas. J. Environ. Manag., 32, 22–45, https://doi.org/10.1080/14486563.2024.2336969, 2025.

Ryan, R. G., Eckert, C., Kelaher, B. P., Harrison, D. P., and Schofield, R.: Boundary layer height above the Great Barrier Reef studied using drone and Mini-Micropulse LiDAR measurements, J. South. Hemisphere Earth Syst. Sci., 74, https://doi.org/10.1071/ES24008, 2024.

Santavy, D. L., Horstmann, C. L., Sharpe, L. M., Yee, S. H., and Ringold, P.: What is it about coral reefs? Translation of ecosystem goods and services relevant to people and their well-being, Ecosphere Wash. DC, 12, 1–27, https://doi.org/10.1002/ecs2.3639, 2021.

Seinfeld, J. H. and Pandis, S. N.: Atmospheric Chemistry and Physics: From Air Pollution to Climate Change, Third., John Wiley & Sons, Inc., Hoboken, New Jersey, 2016.

Sihto, S.-L., Mikkilä, J., Vanhanen, J., Ehn, M., Liao, L., Lehtipalo, K., Aalto, P. P., Duplissy, J., Petäjä, T., Kerminen, V.-M., Boy, M., and Kulmala, M.: Seasonal variation of CCN concentrations and aerosol activation properties in boreal forest, Atmospheric Chem. Phys., 11, 13269–13285, https://doi.org/10.5194/acp-11-13269-2011, 2011.

Stein, A. F., Draxler, R. R., Rolph, G. D., Stunder, B. J. B., Cohen, M. D., and Ngan, F.: NOAA's HYSPLIT Atmospheric Transport and Dispersion Modeling System, Bull. Am. Meteorol. Soc., 96, 2059–2077, https://doi.org/10.1175/BAMS-D-14-00110.1, 2015.

Storelvmo, T., Leirvik, T., Lohmann, U., Phillips, P. C. B., and Wild, M.: Disentangling greenhouse warming and aerosol cooling to reveal Earth's climate sensitivity, Nat. Geosci., 9, 286–289, https://doi.org/10.1038/ngeo2670, 2016.

Sulo, J., Okuljar, M., Alroe, J., Li, Z., Horchler, E. J., Cravigan, L., Miljevic, B., Harrison, L., Harrison, D., Ristovski, Z.: Coral reef emissions enhance aerosol and cloud-condensation nuclei concentrations over the Great Barrier Reef, https://doi.org/10.6084/m9.figshare.30193285.v1, 2025.

Swan, H. B.: The Potential for Great Barrier Reef Regional Climate Regulation via Dimethylsulfide Atmospheric Oxidation Products, Front. Mar. Sci., 9, https://doi.org/10.3389/fmars.2022.869166, 2022.

Swan, H. B., Crough, R. W., Vaattovaara, P., Jones, G. B., Deschaseaux, E. S. M., Eyre, B. D., Miljevic, B., and Ristovski, Z. D.: Dimethyl sulfide and other biogenic volatile organic compound emissions from branching coral and reef seawater: potential sources of secondary aerosol over the Great Barrier Reef, J. Atmospheric Chem., 73, 303–328, https://doi.org/10.1007/s10874-016-9327-7, 2016.

https://doi.org/10.5194/ar-2026-9
Preprint. Discussion started: 16 February 2026


Tessendorf, S. A., Weeks, C. E., Axisa, D., and Bruintjes, R. T.: Aerosol characteristics observed in southeast Queensland and implications for cloud microphysics, J. Geophys. Res. Atmospheres, 118, 2858–2871, https://doi.org/10.1002/jgrd.50274, 2013.

Vaattovaara, P., Swan, H. B., Jones, G. B., Deschaseaux, E., Miljevic, B., Laaksonen, A., and Ristovski, Z. D.: The Contribution of Sulfate and Oxidized Organics in Climatically Important Ultrafine Particles at a Coral Reef Environment, https://doi.org/10.5281/zenodo.1092156, 2014.

Yang, L. and Shami, A.: On hyperparameter optimization of machine learning algorithms: Theory and practice, Neurocomputing, 415, 295–316, https://doi.org/10.1016/j.neucom.2020.07.061, 2020.

Zhao, W., Huang, Y., Siems, S., and Manton, M.: A characterization of clouds over the Great Barrier Reef and the role of local forcing, Int. J. Climatol., 42, 6647–6664, https://doi.org/10.1002/joc.7660, 2022.

Zhao, W., Huang, Y., Siems, S., Manton, M., and Harrison, D.: Interactions between trade wind clouds and local forcings over the Great Barrier Reef: a case study using convection-permitting simulations, Atmospheric Chem. Phys., 24, 5713–5736, https://doi.org/10.5194/acp-24-5713-2024, 2024.